

Revisiting Pre-training in Audio-Visual Learning

Ruoxuan Feng¹, Wenke Xia¹, Di Hu^{1,*}

¹Gaoling School of Artificial Intelligence, Renmin University of China, Beijing
fengruox@gmail.com, {xiawenke2022, dihu}@ruc.edu.cn

Abstract

Pre-training technique has gained tremendous success in enhancing model performance on various tasks, but found to perform worse than training from scratch in some uni-modal situations. This inspires us to think: are the pre-trained models always effective in the more complex multi-modal scenario, especially for the heterogeneous modalities such as audio and visual ones? We find that the answer is No. Specifically, we explore the effects of pre-trained models on two audio-visual learning scenarios: cross-modal initialization and multi-modal joint learning. When cross-modal initialization is applied, the phenomena of “dead channel” caused by abnormal Batchnorm parameters hinders the utilization of model capacity. Thus, we propose Adaptive Batchnorm Re-initialization (ABRi) to better exploit the capacity of pre-trained models for target tasks. In multi-modal joint learning, we find a strong pre-trained uni-modal encoder would bring negative effects on the encoder of another modality. To alleviate such problem, we introduce a two-stage Fusion Tuning strategy, taking better advantage of the pre-trained knowledge while making the uni-modal encoders cooperate with an adaptive masking method. The experiment results show that our methods could further exploit pre-trained models’ potential and boost performance in audio-visual learning. The source code is available at <https://github.com/GeWu-Lab/Revisiting-Pre-training-in-Audio-Visual-Learning>

1. Introduction

Pre-training technique promotes the development of deep learning and achieves promising results in many fields, such as computer vision [17,62], acoustic processing [9,63] and natural language processing [46,47]. The ability to extract features and encode representations learned on large-scale pre-training datasets is proved to be useful in the target

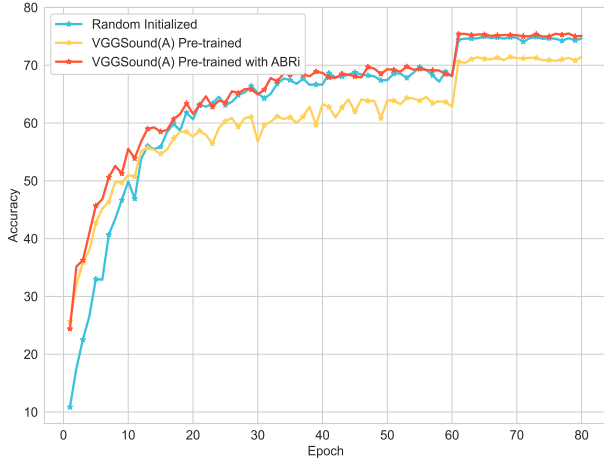
task with a smaller scale of training samples [41,59]. However, when given stronger data augmentation [66], more training samples [22,66] or different target tasks [22,35,66], researchers found that training from scratch occasionally outperforms training from pre-trained models, which implies pre-trained models could not always be profitable.

In fact, the above findings are almost based on uni-modal scenarios. These lead to our way of thinking: for the much more complex multi-modal scenario, is the effectiveness of pre-trained models always held? To answer this, we choose to focus on a pair of typical heterogeneous modalities, audio and visual modality, where the heterogeneous data format is considered to bring more chances in exploring the effectiveness of pre-trained models. Concretely, we concentrate on two typical cases of audio-visual learning [57]: *cross-modal initialization* and *multi-modal joint learning*.

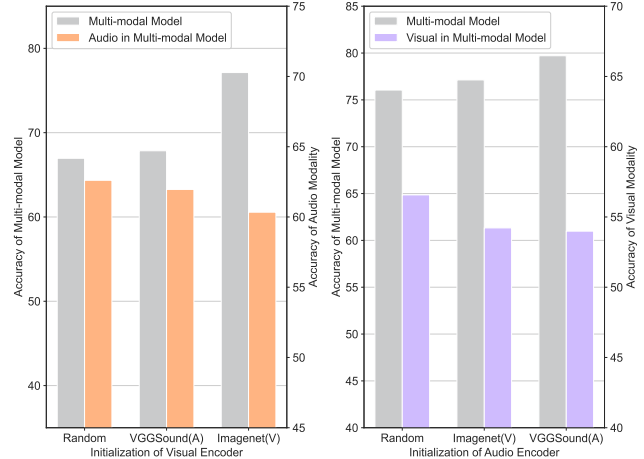
Cross-modal initialization is a technique used when a specific pre-trained model of the target modality could be hard to access. It employs the parameters of a pre-trained model of one modality as the initialization of the model for another modality [55]. According to previous works, cross-modal initialization could improve model performance of the target modality, benefiting from the knowledge learned from another modality [4,31,42]. These works empirically found that the filters of CNNs learned from one modality could be reused in target tasks of another modality to some extent, thus facilitating the learning of the model in target tasks. For example, the edge-aware filters in visual pre-trained model could help to detect the shape or edge in audio spectrograms [42]. *However, we find that the above reuse might not always bring performance gain in the target task, or is even worse than training from scratch, which is surprisingly contrary to common sense, as shown in Fig. 1(a).* Through multiple experiments, we point out that such phenomenon is brought by abnormal *Batch Normalization* (Batchnorm) [27] parameters in widely used ConvBN-ReLU modules, which create “dead channels¹” and hinder the process of fine-tuning. To cope with this problem, we propose *Adaptive Batchnorm Re-initialization* (ABRi)

¹Dead channel indicates the channel that is almost inactivated regardless of the input sample.

* Corresponding author.



(a) Accuracy of the models on CIFAR-100.



(b) Accuracy of uni-modal and multi-modal models on Kinetics-Sounds.

Figure 1. **Underutilization of pre-trained model in audio-visual learning.** (a) Performance of random initialized model, VGGSound [8] pre-trained model and VGGSound pre-trained model with ABRi on CIFAR-100 testing set. (b) Performance of multi-modal models and linear-probing [2] results of uni-modal encoders in the multi-modal model. One modality uses different initialization while the other employs the same ImageNet pre-trained model on Kinetics-Sounds [5] testing set.

to offset the negative effect of abnormal Batchnorm parameters, which adaptively modifies each Batchnorm layer with additional initialized Batchnorm parameters. The experiment results prove that ABRi accelerates the convergence speed and improves the performance when employing pre-trained model, as shown in Fig. 1(a).

Multi-modal joint learning is to train the encoders of different modality in the same framework simultaneously. In recent years, pre-training the uni-modal encoders of the multi-modal model on large-scale datasets (e.g., ImageNet [12] and AudioSet [16]) then fine-tuning the model on multi-modal target tasks [29, 32, 54], has become a dominant paradigm. Fine-tuning the pre-trained uni-modal encoders jointly in a multi-modal setting could achieve better performance [21, 61]. However, little attention has been drawn to the possible negative impact between the encoders, which is brought by introducing the pre-trained uni-modal encoder for the multi-modal model. *Concretely, we find that the representation quality of one modality in the multi-modal model drops, when a stronger pre-trained encoder is applied to the other modality, as shown in Fig. 1(b).* This interesting phenomenon indicates the uni-modal encoder could not fully exploit the knowledge obtained from the pre-training dataset. In order to perform effective cooperation among multiple uni-modal encoders while retaining their representation quality as much as possible, we propose a two-stage Fusion Tuning strategy. In the first stage, we individually fine-tune the uni-modal encoders to fully tap the potential of the pre-trained models. Then, in the second stage, we jointly fine-tune both encoders within the whole model, by adaptively performing sample-wise mask-

ing mechanism over each modality for better cooperation. Using such Fusion Tuning strategy, we could achieve performance improvement on various audio-visual datasets.

We consider that the abnormal Batchnorm parameters and the drop in uni-modal representation quality are two aspects of the underutilization of pre-trained models, which could simultaneously hurt the performance of audio-visual learning. Hence, the proposed ABRi is combined with the Fusion Tuning strategy, which could jointly boost the performance of the multi-modal model further. More conducted experiments also shows that the proposed methods could promote more general learning scenario. To summarize, we find that **the underutilization of not only model capacity, but also model knowledge limits the potential of the pre-trained model** in the multi-modal scenario. We hope these findings could inspire future works.

2. Related works

2.1. Pre-training and fine-tuning

Researchers have come to recognize the effectiveness and potential of pre-trained models since the birth of the pre-training technique [13, 15, 24]. Armed with the models pre-trained on large-scale datasets, recent works have achieved surprising results in computer vision [17, 62], acoustic processing [9, 63] and natural language processing [46, 47]. The knowledge from pre-training datasets could be helpful even when faced with data in different domains [41] or different tasks [18]. However, recent works also found the limitation of pre-trained models. He *et al.* [22] demonstrated that although ImageNet pre-training

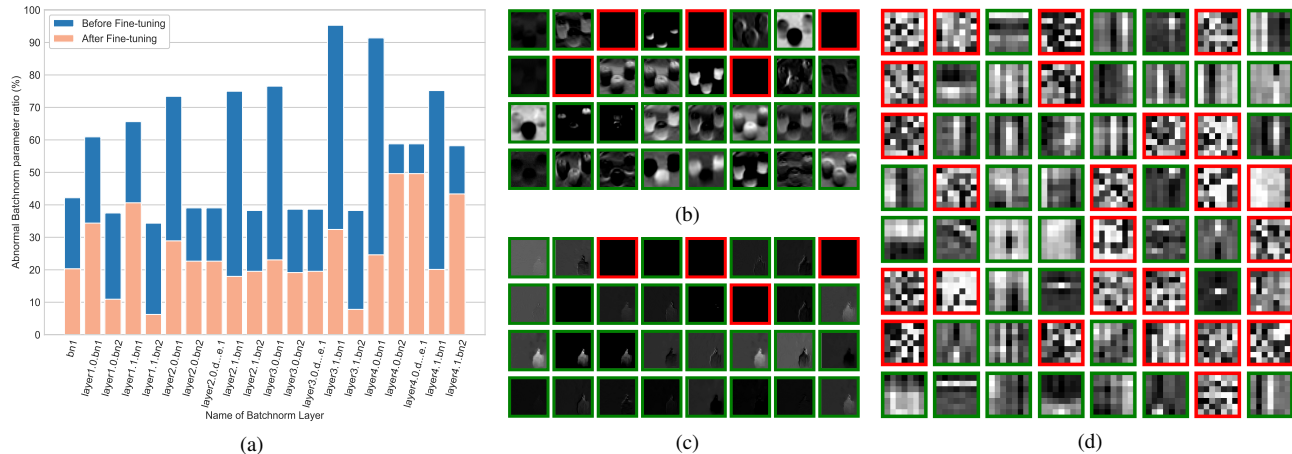


Figure 2. **Visualization of dead channels phenomenon in ResNet-18.** (a) Abnormal parameter ($< 10^{-10}$) ratio of each Batchnorm layer in VGGSound pre-trained model before and after fine-tuned on CIFAR-100 dataset. (b) Feature maps after the first Conv-BN-ReLU in ImageNet pre-trained model. The feature maps of the channels marked with red boxes in the figure are dead features and the corresponding Batchnorm parameters are smaller than 2×10^{-5} . This phenomenon is not unique to particular samples or classes, but exists for most samples. More examples are in *Supp. Materials*. (c) Feature maps of optical flow after the first Conv-BN-ReLU in ImageNet pre-trained model fine-tuned on UCF-101 [51]. The channels with red boxes are remained dead channels. (d) Filters of the first convolutional layer in VGGSound pre-trained model. The Batchnorm parameters corresponding to the filters marked with red boxes are smaller than 10^{-40} .

could accelerate convergence, it fails to improve the performance on a much different task. Zoph *et al.* [66] found that pre-training may hurt performance when stronger augmentation is used during fine-tuning. These works analyzed the effectiveness of pre-training mainly in computer vision. In this paper, we focus on the potential limitation of pre-trained models fine-tuned on cross-modal and multi-modal tasks, which is rarely explored before.

2.2. Cross-modal initialization

Cross-modal initialization is a method that employs the pre-trained model of one modality as the initialization for the model of another modality. Previous works have proved that models pre-trained on large-scale datasets could provide a good initial point even if the modality of the target task is obviously different from the pre-training modality [6, 19, 26, 42, 54]. When a specific pre-trained model of one modality is hard to access (*e.g.*, audio and optical flow), it could be a potential choice to employ the easy-to-access pre-trained model of another modality (*e.g.*, visual [49]). Accordingly, many recently proposed methods use ImageNet pre-trained model as the backbone for audio modeling and achieved considerable improvements [19, 30, 54]. Van Horn *et al.* [54] also used ImageNet pre-trained models as the initialization of audio pre-training. Attempting to explore why cross-modal initialization works even when the modalities are heterogeneous like audio and visual, preliminary research found that the well-trained edge-aware filters in the initial layers of ImageNet pre-trained models could be reused in audio related tasks [42]. These works demon-

strate that the knowledge of the pre-trained model could still be helpful in the target task of another modality. However, they did not investigate whether the capacity of pre-trained models is fully exploited, which is explored in our work.

2.3. Multi-modal joint learning

A typical training paradigm in various multi-modal (*e.g.*, audio-visual) tasks is to use the information of both modalities simultaneously and fuse them to make prediction during the training phase [25, 34]. Many multi-modal learning methods have been proposed to efficiently fuse the information in different levels, such as early fusion [7, 48] and late fusion [3, 44]. Hybrid fusion methods in multiple levels and with well-designed interactions further improve the performance of multi-modal joint learning [10, 39].

Aside from the fusion methods, some multi-modal joint learning mechanisms have been proposed to better train multi-modal networks. Wang *et al.* [56] found that the uni-modal over-fitting problem could degrade the performance of the joint model, then proposed Gradient-Blending across modalities to alleviate this problem. Peng *et al.* [43] proposed an on-the-fly gradient modulation strategy to regulate the gradients of each uni-modal encoder dynamically. These works mainly focus on the cooperation between different modalities. However, they did not discuss the impact on cooperation, caused by applying well pre-trained encoders. In this work, we focus on exploring the influence between the uni-modal encoders when employing pre-training technique, then propose a two-stage Fusion Tuning strategy to reduce the impact.

3. Cross-modal initialization

3.1. Underutilization of model capacity

Batch Normalization (Batchnorm) has been widely adopted to improve the speed and stability of training deep neural networks [27]. By introducing Batchnorm into convolutional neural network (CNN) and combining it with convolutional layer (Conv) and ReLU activation, the structure of Conv-BN-ReLU has become a general module in deep convolutional networks [11, 23, 28]. Specifically, the k -th channel of the Batchnorm layer essentially normalizes the k -th feature maps $x_k \in \mathbb{R}^{M \times H \times W}$ produced by the previous convolutional layer within M mini-batch. The normalized feature maps \hat{x}_k of the k -th channel are then scaled via γ_k and shifted via β_k to obtain the final output y_k as

$$y_k = \gamma_k \hat{x}_k + \beta_k, \quad (1)$$

where γ_k and β_k are trainable parameters aiming to maintain the representation power of the network [27].

However, we discover that the absolute value of some parameter pairs ($|\gamma_k|$, $|\beta_k|$) is significantly smaller than other parameters, after checking all the Batchnorm layers in VGGSound [8] and ImageNet [12] pre-trained ResNet-18 [23] models. In Fig. 2(a), blue bars indicate that these abnormal Batchnorm parameters could be found in every Batchnorm layer inside VGGSound pre-trained model. The abnormal ratio is even higher than 90% in some layers. This unusual phenomenon attracts us to explore its impact on fine-tuning, especially when performing cross-modal initialization.

During feedforward, if $|\gamma_k|$ and $|\beta_k|$ are too small, the mean and variance of the corresponding feature maps are adjusted to tiny values due to Eq. (1). Worse still, in experiments we find that the channels with abnormal Batchnorm parameters are more likely to produce “dead features”² [60] after ReLU. This phenomenon does not merely exist for particular samples or classes but for most samples, indicating the channels are hard to be activated, as shown in Fig. 2(b). We name these channels as “dead channels”. The model performance could be limited if these dead channels remain after fine-tuning, as shown in Fig. 2(c), for the corresponding feature maps provide less information to the next layer, causing information loss [36, 37].

During feedback, gradients back-propagated through Batchnorm layers are associated with the scaling parameter γ_k ³:

$$\begin{aligned} \frac{\partial \mathcal{L}}{\partial x_{k,m}} &= \frac{\partial \mathcal{L}}{\partial \hat{x}_{k,m}} \cdot \frac{1}{\sqrt{\sigma_k^2}} + \frac{\partial \mathcal{L}}{\partial \sigma_k^2} \cdot \frac{2(x_{k,m} - \mu_k)}{M} + \frac{\partial \mathcal{L}}{\partial \mu_k} \cdot \frac{1}{M} \\ &\propto \frac{\partial \mathcal{L}}{\partial \hat{x}_{k,m}} \\ &= \frac{\partial \mathcal{L}}{\partial y_{k,m}} \cdot \gamma_k, \end{aligned} \quad (2)$$

²Dead features are feature maps with all zero entries.

³ β_k has less impact in feedback phase.

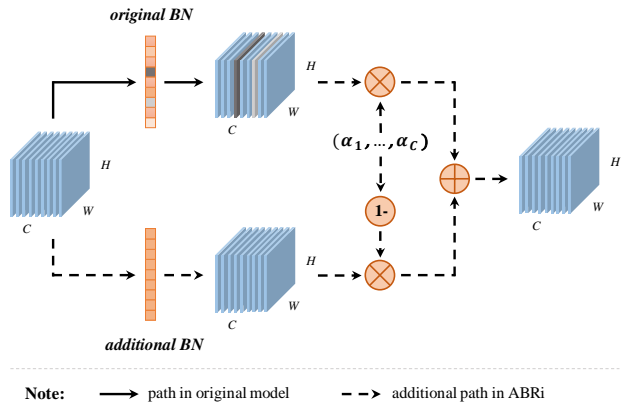


Figure 3. The pipeline of Adaptive Batchnorm Re-initialization (ABRi). The grey blocks in original Batchnorm layer indicate the channels with abnormal parameters.

where \mathcal{L} is the loss function and m indicates the index of the feature map within M mini-batch. According to Eq. (2), $\frac{\partial \mathcal{L}}{\partial x_{k,m}}$ is proportional to γ_k . This indicates that the abnormal γ_k slows down the back-propagation of gradients. Thus, the corresponding filters in Conv-BN-ReLU structure are difficult to be updated. As shown in Fig. 2(d), the filters marked with red boxes are obviously under-optimized.

Based on the above analysis, the abnormal Batchnorm parameters could bring potential problem during fine-tuning. Practically, the parameters of the pre-trained model require to adapt to the target task [41, 42, 59]. Still, the abnormal parameters limit the update of some channels, resulting in the underutilization of the model capacity. For the more challenging paradigm of cross-modal initialization, the model requires more tuning for a different modality. Directly fine-tuning the pre-trained model in cross-modal scenario, we find the ratio of abnormal parameters could reduce to some extent, but still remains a high percentage, as the shown orange bars in Fig. 2(a) and the red boxes in Fig. 2(c). Hence, a kind of effective fine-tuning strategy is highly expected to reactivate all the “dead channels”, then fully release the model capacity for the target task.

3.2. Adaptive Batchnorm Re-initialization

To cope with the dead channel problem caused by the abnormal Batchnorm parameters, one naive strategy is to directly re-initialize every abnormal pair (γ_k , β_k) to (1, 0) before training. However, this strategy could damage the target distribution of feature maps and affect the coordination with the next layer. To minimize the negative impact of abnormal parameters while ensuring coordination, an additional initialized Batchnorm layer is adaptively combined with each original Batchnorm layer. Specifically, the feature maps of the k -th channel go through the above two Batch-

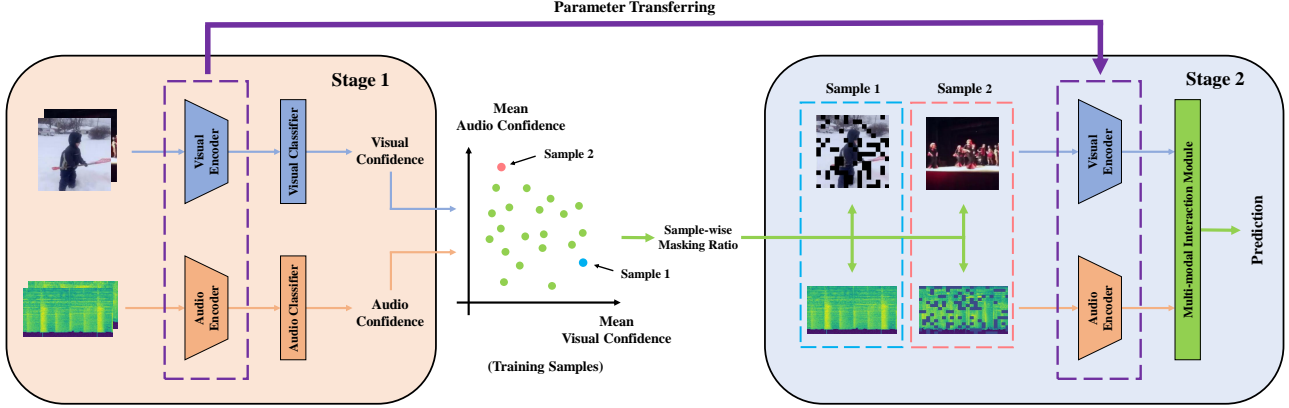


Figure 4. **The pipeline of two-stage Fusion Tuning strategy.** In stage 1, we separately train the uni-modal encoders and record the confidence of each training sample on both modalities. The sample-wise masking ratio is then calculated by the mean confidence of the sample on the two modalities. In stage 2, we train the entire multi-modal model consisting of the fine-tuned uni-modal encoders transferred from stage 1 and a multi-modal interaction module (e.g., a joint classifier). During the training process, we mask some parts of the easy-to-learn training sample of one modality based on the sample-wise masking ratio.

norm layers simultaneously:

$$y_k = \alpha_k \cdot BN_{ori}(x_k) + (1 - \alpha_k) \cdot BN_{add}(x_k), \quad (3)$$

where BN_{ori} is the original Batchnorm layer, BN_{add} is the additional Batchnorm layer and α_k is a trainable parameter to balance each original and additional channel. The pipeline is illustrated in Fig. 3. The new Batchnorm layers help to reactivate the dead channels in the pre-trained model then the capacity of the model could be better utilized.

The total amount of the additional parameters is $1.5 \times$ total BN parameters of the original model, which will not increase GPU memory occupation evidently. Furthermore, this method is not restricted to a particular modality and could be used in different modalities.

4. Multi-modal joint learning

4.1. Underutilization of model knowledge

Although introducing a stronger pre-trained encoder for one modality in the multi-modal model is very likely to improve the performance, we find that this could damage the representation ability of the other. As shown in Fig. 1(b), both of the uni-modal encoders suffer a performance drop after introducing a stronger pre-trained model for another modality, indicating that both of the pre-trained encoders could have not yet adapted to the target task and thoroughly exploited the knowledge from the pre-trained model.

The above phenomenon indicates that the encoder of one modality could influence the learning of other encoder when performing joint training. Recent work preliminarily pointed out that high-quality predictions of one modality could reduce the gradient back-propagated to another en-

coder [43], thus the optimization of the corresponding encoder could be insufficient and the representation quality could be reduced. When directly initializing encoder with pre-trained model, predictions with high quality could be produced on the samples of one modality at the beginning, which are considered to be easy-to-learn. This could further exacerbate the above problem, making the encoders hard to effectively adapt to the target task and utilize task-oriented knowledge from pre-trained model. Hence, how to coordinate the encoders while better utilizing the knowledge of the pre-training dataset for target task is a meaningful problem.

4.2. Two-stage Fusion Tuning

In order to address the above problem, we divide the process of joint training based on pre-trained models into two stages: separately training the uni-modal encoders then cooperatively fine-tuning the multi-modal network. The whole pipeline is shown in Fig. 4.

In the first stage, to avoid the potential negative impact among modalities, we divide the multi-modal model into separated uni-modal ones, then fine-tune them on their own uni-modal dataset detached from the multi-modal dataset. This stage aims to make both of the encoders sufficiently exploit task-oriented knowledge for each modality.

In the second stage, the fine-tuned uni-modal encoders are assembled with a multi-modal interaction module to form the complete multi-modal model. The purpose of this stage is to perform effective cooperation among the separately trained encoders. However, the optimization of the multi-modal network, especially the interaction module, is still influenced by the easy-to-learn samples of one modality, reducing the cooperation quality.

Inspired by the data augmentation technique of adding

Pre-training dataset	Audio tasks			Visual tasks	
	ESC50	TUT AS 2016	Kinetics-Sounds	Cifar-100	Caltech-256
Random	77.95	62.78	54.56	75.31	48.09
ImageNet (V)	89.35	72.10	62.07	79.97	77.55
VGGSound (A)	90.35	73.89	63.53	72.54	47.00
ImageNet (V)†	89.95 (+0.60)	73.02 (+0.92)	62.53 (+0.46)	80.12 (+0.15)	77.86 (+0.31)
VGGSound (A)†	92.75 (+2.40)	75.37 (+1.48)	63.80 (+0.27)	75.58 (+3.06)	49.69 (+2.69)

Table 1. Comparison of performance with and without ABRi on different uni-modal datasets. † indicates ABRi is applied.

noise [1, 40], we propose to randomly mask some parts of the easy-to-learn samples. This strategy could lower the confidence on the easy-to-learn sample of one modality, reinforcing the learning of the hard-to-learn sample of the other modality and improving cooperating quality. To obtain the learning difficulties of training samples on two modalities, we record the confidence of each training sample in every epoch of the first stage. We then calculate the mean confidence of each sample for each modality, which could reflect the modality-wise difficulty of learning to some extent. [52]. The masking ratio $\{m_i^a, m_i^v\}$ of the input $\{x_i^a, x_i^v\}$ is then calculated by

$$\begin{aligned}
 m_i^a &= \begin{cases} \rho^a \cdot \tanh[\eta^a \cdot (c_i^a - c_i^v)] & c_i^a > c_i^v \text{ and } c_i^v > t \\ 0 & \text{others,} \end{cases} \\
 m_i^v &= \begin{cases} \rho^v \cdot \tanh[\eta^v \cdot (c_i^v - c_i^a)] & c_i^v > c_i^a \text{ and } c_i^a > t \\ 0 & \text{others,} \end{cases}
 \end{aligned} \quad (4)$$

where $\{c_i^a, c_i^v\}$ is the mean confidence of the sample on two modalities, $\{\rho^a, \rho^v\}$ and $\{\eta^a, \eta^v\}$ are parameters to control the range of masking ratio and t is a hyper-parameter to avoid masking the sample of one modality when the confidence on the other modality is apparently low (more likely to be noise). Our proposed ABRi technique in Sec. 3.2 could be applied to the encoders in both stages, then the integrated method could further improve the performance of multi-modal joint learning.

5. Experiments

5.1. Datasets

Pre-training datasets. We select three widely used large-scale datasets: ImageNet-1K [12] (1.28M samples) VGGSound [8] (200K samples) and AudioSet [16] (2.08M samples) to pre-train our models. ImageNet-1K is the pre-training dataset for visual modality, while VGGSound and AudioSet are pre-training datasets for audio modality.

Uni-modal datasets. For audio modality, we use ESC-50 [45] and TUT Acoustic Scenes 2016 [38] datasets. For visual modality, CIFAR-100 [33] and Caltech-256 [20] are selected to be the target datasets. We also extract the audio modality from Kinetics-Sounds [5] as a uni-modal dataset.

Multi-modal datasets. For multi-modal tasks, Kinetics-Sounds, AVE [53] and UCF-101 [51] are chosen. We also randomly select a subset of VGGSound, where the amount of samples per class is 90,10,30 in training, validation and testing set. Totally, it contains 27,810 training samples, 3,090 validation samples and 9,270 testing samples. The amount of samples in each class is apparently lower than the number of classes, which could facilitate the evaluation on the utilization of pre-trained knowledge.

5.2. Experimental settings

In our experiments, we employ ResNet-18 as the CNN backbones. For audio modality, we convert each 10-second audio waveform into 128-dimensional log Mel filterbank features using a window size of 25ms as [19] does. Audio clips shorter than 10s are duplicated several times along the time axis and cut into 10s. The obtained 128×1024 spectrogram is then duplicated three times to create a 3-channel input for the CNN network. In audio uni-modal tasks, we apply time mask and frequency mask. For the visual modality in multi-modal tasks, we extract frames of each video clip with 1 fps. Each video clip is averagely divided into 3 segments. Then, we randomly take 1 frames from each segment and put them into the 2D network as [64] does.

5.3. Evaluation of ABRi on uni-modal tasks

To evaluate the effectiveness of ABRi, we conduct experiments on several uni-modal datasets. From the results in Tab. 1, we could obtain four observations. Firstly, the pre-trained model of one modality is more effective in target tasks with the same modality. Concretely, the ImageNet pre-trained model outperforms the VGGSound pre-trained model on visual target tasks, while the result is the opposite on audio tasks. Secondly, consistent performance improvement proves the effectiveness of ABRi. In addition, more notable improvements are visible in VGGSound pre-trained model, which has more abnormal Batchnorm parameters. Thirdly, the improvement is more evident when performing cross-modal initialization. This phenomenon corresponds to the analysis in Sec. 3.1. Specifically, the underutilization of model capacity brings more impact in the case of

Dataset	Pre-train (Audio)	Accuracy			mAP		
		DF	JT	FusT	DF	JT	FusT
VGGs	AudioSet	49.90	52.61	52.78	50.41	55.67	55.89
	ImageNet	46.93	48.99	49.62	47.33	50.77	52.04
KS	VGGSound	76.01	79.13	81.29	81.98	85.92	87.23
	AudioSet	79.13	81.02	83.90	84.82	88.03	90.20
	ImageNet	73.62	74.93	77.59	79.88	81.23	84.47

Table 2. Comparison with decision fusion and vanilla joint training on Kinetics-Sounds (KS) and VGGSound subset (VGGs). Visual encoders are pre-trained on ImageNet. DF means decision fusion, JT means joint training and FusT means our Fusion Tuning strategy.

	Pre-train (Audio)	FusT*	FusT*-lr	FusT-mean	OGM-GE [43]	G-Blending [56]	FusT
Acc	VGGSound	81.13	80.94	80.98	79.44	80.02	81.29
	AudioSet	83.52	83.37	83.13	80.79	83.29	83.90
	ImageNet	74.82	75.20	75.93	75.66	76.93	77.59
mAP	VGGSound	87.24	87.38	87.06	86.24	86.74	87.23
	AudioSet	90.15	89.91	89.82	88.41	90.08	90.20
	ImageNet	81.97	82.47	82.55	82.57	84.36	84.47

Table 3. Comparison with variants of FusT and two modulation strategies on Kinetics-Sounds. Visual encoders are pre-trained on ImageNet. FusT*, FusT*-lr and FusT-mean are three variants of FusT strategy. * indicates masking strategy is not applied in the second stage.

cross-modal initialization. Our proposed ABRI reactivates the dead channels and alleviates this problem. Finally, it is noteworthy that the VGGSound pre-trained model with ABRI outperforms the model trained from scratch on visual datasets. Although it does not exceed the ImageNet pre-trained model having the same modality with the target task, this result demonstrates the knowledge from the audio modality could be helpful in the target task of visual modality with more informative features.

5.4. Evaluation of Fusion Tuning strategy

To evaluate the effect of our *Fusion Tuning strategy* (FusT), we compare it with *decision fusion* (DF) and *vanilla joint training* (JT). In decision fusion, we average the softmax score of two modalities following [50]. The result in Tab. 2 shows a superior performance of our method among all pairs of pre-trained encoder on both datasets, demonstrating the effectiveness of our Fusion Tuning strategy.

In order to show the advantage of the simple-wise masking strategy, we compare the Fusion Tuning strategy with three variants: (1) *Fusion Tuning without masking* (FusT*), (2) *Fusion Tuning without masking but with modality-specific learning rate*⁴ (FusT*-lr) and (3) *Fusion Tuning with modality-wise masking ratio*⁵ (FusT-mean). It is to be

⁴We set the learning rate of audio encoders 0.5 times to visual encoders.

⁵We compute the mean of the masking ratio for each modality and all the inputs of one modality share the same masking ratio.

mentioned that the last two variants are modality-wise modulation methods, while ours is a more fine-grained sample-wise method. As shown in Tab. 3, our method outperforms all the variants on accuracy and most of the mAP. The accuracy of the models with AudioSet and VGGSound pre-trained audio encoder even dropped in FusT*-lr and FusT-mean variants, compared with Fusion Tuning without masking. This indicates that these easy but coarse variant strategies are not stable, demonstrating the meaning and advantage of our sample-wise modulation method.

We also make a comparison with two existing imbalance modulation strategies: OGM-GE [43] and Gradient-Blending [56]. OGM-GE is a batch-wise modulation strategy that dynamically regulates the gradient of uni-modal encoders based on the prediction within the mini-batch. Gradient-Blending is a modality-wise strategy that introduces additional uni-modal losses and adaptively modulates their weights. As shown in Tab. 3, our Fusion Tuning strategy shows superior performance among these methods. The above methods mainly focus on the cooperation between the two modalities, while less considering the utilization of model knowledge of each uni-modal encoder. This indicates that the existing batch-wise and modality-wise methods could be less effective in handling the underutilization of model knowledge. In contrast, our sample-wise method exploits more potential of pre-trained models.

Strategy	Pre-train (Audio)	Acc	mAP
FusT	VGGSound	81.29	87.23
	AudioSet	83.90	90.20
	ImageNet	77.59	84.47
FusT†	VGGSound	81.48	87.34
	AudioSet	84.14	89.99
	ImageNet	77.90	84.50
FusT‡	VGGSound	77.51	83.81
	AudioSet	83.63	90.03
	ImageNet	77.63	83.98

Table 4. Comparison of performance with and without ABRi on Kinetics-Sounds. Visual encoders are pre-trained on ImageNet. † indicates ABRi is applied on visual encoders. ‡ indicates that ABRi is applied on both encoders.

5.5. Combination and extension of the two methods

Based on the two aspects of underutilization of pre-trained models, model capacity and model knowledge, we combine ABRi with Fusion Tuning strategy and apply them on Kinetics-Sounds dataset. Specifically, we conduct an experiment on Kinetics-Sounds dataset, comparing the performance of the multi-modal model without ABRi, the model with ABRi on visual encoder and the model with ABRi on both encoders. The slight boosts on the model with ABRi only on visual encoder shown in Tab. 4 demonstrate that the dead channels hurt the performance to some extent, but the underutilization of model knowledge is the critical reason for the limited performance on Kinetics-Sounds. Surprisingly, the performance of the models drops when ABRi is also applied on audio encoders. In Kinetics-Sounds, audio samples are generally more easy-to-learn than visual samples. As a result, the optimization of the multi-modal model is dominated by audio modality, leading to under-optimization of visual modality [14,43]. The experiment result indicates that simply improving the representation quality of the dominant modality (such as audio in this case) could aggravate the under-optimization problem of the other modality and hurt the performance in some situations. This severe problem could increase the difficulty of modulation, and is worthy of exploration in future works.

Extending to more complex interaction modules. We apply the two-stage Fusion Tuning strategy on two representative frameworks of audio-visual event localization task: Audio-Guided Visual Attention (AGVA) [53] and Positive Sample Propagation (PSP) [65] for AVE dataset. Since audio-visual event localization is a more fine-grained task, these frameworks have well-designed cross-modal interaction mechanisms. Hence, we extract the parts only relevant to a single modality and train them in the first stage. In addition, we apply ABRi on both uni-modal encoders, for AVE

Framework	Strategy	Pre-train (Audio)	Acc
AGVA [53]	JT	VGGSound	69.15
		ImageNet	67.41
	FusT‡	VGGSound	72.64
		ImageNet	68.41
PSP [65]	JT	VGGSound	73.38
		ImageNet	68.41
	FusT‡	VGGSound	74.13
		ImageNet	71.89

Table 5. Comparison on AVE dataset with and without Fusion Tuning strategy and ABRi methods in two frameworks. Visual encoders are pre-trained on ImageNet. ‡ indicates that ABRi is applied on both encoders.

Strategy	Accuracy	mAP
Decision Fusion	81.49	86.49
Joint Training	78.93	84.70
Fusion Tuning‡	83.62	89.00

Table 6. Performance of the model with two-stage Fusion Tuning strategy and ABRi on UCF-101. Encoders are pre-trained on ImageNet. ‡ indicates that ABRi is applied on both encoders.

dataset is a more balanced dataset. The complete model is then fine-tuned in the second stage based on the confidence recorded in the first stage. The comparison results are shown in Tab. 5. The improvement demonstrates that our Fusion Tuning strategy could be applicable with more complex interaction modules.

Extending to other modalities. To demonstrate the generality of our methods on other modalities, we conduct an experiment on UCF-101 dataset. The two modalities are RGB and optical flow, which are less heterogeneous than audio and visual. The models for optical flow modality often use ImageNet pre-trained model as initialization, which could be influenced by the dead channels as well. The performance gain shown in Tab. 6 indicates the universality of our methods for different modalities.

6. Discussion

In this paper, we find that the underutilization of model capacity and model knowledge limits the potential of pre-trained models in two typical cases of audio-visual learning and analyze their causes. We propose Adaptive Batchnorm Re-initialization (ABRi) and two-stage Fusion Tuning strategy to better utilizing the pre-trained models in both cases.

Meanings of cross-modal initialization. Although the VGGSound pre-trained model with ABRi outperforms

training from scratch on visual tasks, it is left behind by the ImageNet pre-trained model. Our experiment is only an attempt and we do not recommend using the pre-trained model from another less informative modality if the pre-trained model of its modality exists. However, if the pre-trained model is hard to access, cross-modal initialization will become a good choice other than training from scratch.

Limitation. Although our methods improve the performance of pre-trained models in uni-modal and multi-modal tasks, they require additional GPU memory and more training epochs. The purposed ABRi could contribute less for the model with few abnormal Batchnorm parameters.

References

- [1] Aida Ahmadzadegan, Petar Simidzija, Ming Li, and Achim Kempf. Neural networks can learn to utilize correlated auxiliary noise. *Scientific reports*, 11(1):1–8, 2021. 6
- [2] Guillaume Alain and Yoshua Bengio. Understanding intermediate layers using linear classifier probes. *arXiv preprint arXiv:1610.01644*, 2016. 2, 12
- [3] Mohammad Rafiqul Alam, Mohammed Bennamoun, Roberto Togneri, and Ferdous Sohel. A confidence-based late fusion framework for audio-visual biometric identification. *Pattern Recognition Letters*, 52:65–71, 2015. 3
- [4] Shahin Amiriparian, Maurice Gerczuk, Sandra Ottl, Lukas Stappen, Alice Baird, Lukas Koebe, and Björn Schuller. Towards cross-modal pre-training and learning tempo-spatial characteristics for audio recognition with convolutional and recurrent neural networks. *EURASIP Journal on Audio, Speech, and Music Processing*, 2020(1):1–11, 2020. 1
- [5] Relja Arandjelovic and Andrew Zisserman. Look, listen and learn. In *Proceedings of the IEEE International Conference on Computer Vision*, pages 609–617, 2017. 2, 6, 16
- [6] Joao Carreira and Andrew Zisserman. Quo vadis, action recognition? a new model and the kinetics dataset. In *proceedings of the IEEE Conference on Computer Vision and Pattern Recognition*, pages 6299–6308, 2017. 3
- [7] Ginevra Castellano, Loic Kessous, and George Caridakis. Emotion recognition through multiple modalities: face, body gesture, speech. In *Affect and emotion in human-computer interaction*, pages 92–103. Springer, 2008. 3
- [8] Honglie Chen, Weidi Xie, Andrea Vedaldi, and Andrew Zisserman. Vggsound: A large-scale audio-visual dataset. In *ICASSP 2020-2020 IEEE International Conference on Acoustics, Speech and Signal Processing (ICASSP)*, pages 721–725. IEEE, 2020. 2, 4, 6, 14
- [9] Ke Chen, Xingjian Du, Bilei Zhu, Zejun Ma, Taylor Berg-Kirkpatrick, and Shlomo Dubnov. Hts-at: A hierarchical token-semantic audio transformer for sound classification and detection. In *ICASSP 2022-2022 IEEE International Conference on Acoustics, Speech and Signal Processing (ICASSP)*, pages 646–650. IEEE, 2022. 1, 2
- [10] Shizhe Chen and Qin Jin. Multi-modal conditional attention fusion for dimensional emotion prediction. In *Proceedings of the 24th ACM international conference on Multimedia*, pages 571–575, 2016. 3
- [11] François Chollet. Xception: Deep learning with depthwise separable convolutions. In *Proceedings of the IEEE conference on computer vision and pattern recognition*, pages 1251–1258, 2017. 4
- [12] Jia Deng, Wei Dong, Richard Socher, Li-Jia Li, Kai Li, and Li Fei-Fei. Imagenet: A large-scale hierarchical image database. In *2009 IEEE conference on computer vision and pattern recognition*, pages 248–255. Ieee, 2009. 2, 4, 6, 14
- [13] Jacob Devlin, Ming-Wei Chang, Kenton Lee, and Kristina Toutanova. Bert: Pre-training of deep bidirectional transformers for language understanding. *arXiv preprint arXiv:1810.04805*, 2018. 2
- [14] Chenzhuang Du, Tingle Li, Yichen Liu, Zixin Wen, Tianyu Hua, Yue Wang, and Hang Zhao. Improving multi-modal learning with uni-modal teachers. *arXiv preprint arXiv:2106.11059*, 2021. 8
- [15] Dumitru Erhan, Aaron Courville, Yoshua Bengio, and Pascal Vincent. Why does unsupervised pre-training help deep learning? In *Proceedings of the thirteenth international conference on artificial intelligence and statistics*, pages 201–208. JMLR Workshop and Conference Proceedings, 2010. 2
- [16] Jort F Gemmeke, Daniel PW Ellis, Dylan Freedman, Aren Jansen, Wade Lawrence, R Channing Moore, Manoj Plakal, and Marvin Ritter. Audio set: An ontology and human-labeled dataset for audio events. In *2017 IEEE international conference on acoustics, speech and signal processing (ICASSP)*, pages 776–780. IEEE, 2017. 2, 6, 14
- [17] Golnaz Ghiasi, Yin Cui, Aravind Srinivas, Rui Qian, Tsung-Yi Lin, Ekin D Cubuk, Quoc V Le, and Barret Zoph. Simple copy-paste is a strong data augmentation method for instance segmentation. In *Proceedings of the IEEE/CVF Conference on Computer Vision and Pattern Recognition*, pages 2918–2928, 2021. 1, 2
- [18] Ross Girshick, Jeff Donahue, Trevor Darrell, and Jitendra Malik. Rich feature hierarchies for accurate object detection and semantic segmentation. In *Proceedings of the IEEE conference on computer vision and pattern recognition*, pages 580–587, 2014. 2
- [19] Yuan Gong, Yu-An Chung, and James Glass. Ast: Audio spectrogram transformer. *arXiv preprint arXiv:2104.01778*, 2021. 3, 6
- [20] Gregory Griffin, Alex Holub, and Pietro Perona. Caltech-256 object category dataset. 2007. 6, 16
- [21] Daya Guo and Zhaoyang Zeng. Multi-modal representation learning for video advertisement content structuring. In *Proceedings of the 29th ACM International Conference on Multimedia*, pages 4770–4774, 2021. 2
- [22] Kaiming He, Ross Girshick, and Piotr Dollár. Rethinking imagenet pre-training. In *Proceedings of the IEEE/CVF International Conference on Computer Vision*, pages 4918–4927, 2019. 1, 2
- [23] Kaiming He, Xiangyu Zhang, Shaoqing Ren, and Jian Sun. Deep residual learning for image recognition. In *Proceedings of the IEEE conference on computer vision and pattern recognition*, pages 770–778, 2016. 4, 12

- [24] Dan Hendrycks, Kimin Lee, and Mantas Mazeika. Using pre-training can improve model robustness and uncertainty. In *International Conference on Machine Learning*, pages 2712–2721. PMLR, 2019. 2
- [25] Di Hu, Yake Wei, Rui Qian, Weiyao Lin, Ruihua Song, and Ji-Rong Wen. Class-aware sounding objects localization via audiovisual correspondence. *IEEE Transactions on Pattern Analysis and Machine Intelligence*, 44(12):9844–9859, 2021. 3
- [26] Zhaoyang Huang, Xiaoyu Shi, Chao Zhang, Qiang Wang, Ka Chun Cheung, Hongwei Qin, Jifeng Dai, and Hongsheng Li. Flowformer: A transformer architecture for optical flow. *arXiv preprint arXiv:2203.16194*, 2022. 3
- [27] Sergey Ioffe and Christian Szegedy. Batch normalization: Accelerating deep network training by reducing internal covariate shift. In *International conference on machine learning*, pages 448–456. PMLR, 2015. 1, 4, 12
- [28] Mina Jafari, Dorothee Auer, Susan Francis, Jonathan Garibaldi, and Xin Chen. Dru-net: an efficient deep convolutional neural network for medical image segmentation. In *2020 IEEE 17th International Symposium on Biomedical Imaging (ISBI)*, pages 1144–1148. IEEE, 2020. 4
- [29] Aishwarya Kamath, Mannat Singh, Yann LeCun, Gabriel Synnaeve, Ishan Misra, and Nicolas Carion. Mdetr-modulated detection for end-to-end multi-modal understanding. In *Proceedings of the IEEE/CVF International Conference on Computer Vision*, pages 1780–1790, 2021. 2
- [30] Evangelos Kazakos, Arsha Nagrani, Andrew Zisserman, and Dima Damen. Epic-fusion: Audio-visual temporal binding for egocentric action recognition. In *Proceedings of the IEEE/CVF International Conference on Computer Vision*, pages 5492–5501, 2019. 3
- [31] Jaehun Kim. Urban sound tagging using multi-channel audio feature with convolutional neural networks. *Proceedings of the Detection and Classification of Acoustic Scenes and Events*, 2020. 1
- [32] DN Krishna. Using large pre-trained models with cross-modal attention for multi-modal emotion recognition. *arXiv preprint arXiv:2108.09669*, 2021. 2
- [33] Alex Krizhevsky, Geoffrey Hinton, et al. Learning multiple layers of features from tiny images. 2009. 6, 16
- [34] Guangyao Li, Yake Wei, Yapeng Tian, Chenliang Xu, Ji-Rong Wen, and Di Hu. Learning to answer questions in dynamic audio-visual scenarios. In *Proceedings of the IEEE/CVF Conference on Computer Vision and Pattern Recognition*, pages 19108–19118, 2022. 3
- [35] Hengduo Li, Bharat Singh, Mahyar Najibi, Zuxuan Wu, and Larry S Davis. An analysis of pre-training on object detection. *arXiv preprint arXiv:1904.05871*, 2019. 1
- [36] Yudong Liang, Radu Timofte, Jinjun Wang, Yihong Gong, and Nanning Zheng. Single image super resolution-when model adaptation matters. *arXiv preprint arXiv:1703.10889*, 2017. 4
- [37] Parmita Mehta, Aaron Lee, Cecilia Lee, Magdalena Balazinska, and Ariel Rokem. Multilabel multiclass classification of oct images augmented with age, gender and visual acuity data. *bioRxiv*, page 316349, 2018. 4
- [38] Annamaria Mesaros, Toni Heittola, and Tuomas Virtanen. Tut database for acoustic scene classification and sound event detection. In *2016 24th European Signal Processing Conference (EUSIPCO)*, pages 1128–1132. IEEE, 2016. 6, 16
- [39] Arsha Nagrani, Shan Yang, Anurag Arnab, Aren Jansen, Cordelia Schmid, and Chen Sun. Attention bottlenecks for multimodal fusion. *Advances in Neural Information Processing Systems*, 34:14200–14213, 2021. 3
- [40] Tiago S Nazaré, Gabriel B Costa, Welinton A Contato, and Moacir Ponti. Deep convolutional neural networks and noisy images. In *Iberoamerican Congress on Pattern Recognition*, pages 416–424. Springer, 2017. 6
- [41] Behnam Neyshabur, Hanie Sedghi, and Chiyuan Zhang. What is being transferred in transfer learning? *Advances in neural information processing systems*, 33:512–523, 2020. 1, 2, 4
- [42] Kamalesh Palanisamy, Dipika Singhania, and Angela Yao. Rethinking cnn models for audio classification. *arXiv preprint arXiv:2007.11154*, 2020. 1, 3, 4
- [43] Xiaokang Peng, Yake Wei, Andong Deng, Dong Wang, and Di Hu. Balanced multimodal learning via on-the-fly gradient modulation. In *Proceedings of the IEEE/CVF Conference on Computer Vision and Pattern Recognition*, pages 8238–8247, 2022. 3, 5, 7, 8, 12, 14, 15
- [44] AG Amitha Perera, Sangmin Oh, Matthew J Leotta, Ilseo Kim, Byungki Byun, Chin-Hui Lee, Scott McCloskey, Jingchen Liu, Ben Miller, Zhi Feng Huang, et al. Genie trecvid 2011 multimedia event detection: Late-fusion approaches to combine multiple audio-visual features. In *TRECVID*, 2011. 3
- [45] Karol J Piczak. Esc: Dataset for environmental sound classification. In *Proceedings of the 23rd ACM international conference on Multimedia*, pages 1015–1018, 2015. 6, 16
- [46] Alec Radford, Jeffrey Wu, Rewon Child, David Luan, Dario Amodei, Ilya Sutskever, et al. Language models are unsupervised multitask learners. *OpenAI blog*, 1(8):9, 2019. 1, 2
- [47] Colin Raffel, Noam Shazeer, Adam Roberts, Katherine Lee, Sharan Narang, Michael Matena, Yanqi Zhou, Wei Li, Peter J Liu, et al. Exploring the limits of transfer learning with a unified text-to-text transformer. *J. Mach. Learn. Res.*, 21(140):1–67, 2020. 1, 2
- [48] Bjorn Schuller, Dejan Arsic, Gerhard Rigoll, Matthias Wimmer, and Bernd Radig. Audiovisual behavior modeling by combined feature spaces. In *2007 IEEE International Conference on Acoustics, Speech and Signal Processing-ICASSP'07*, volume 2, pages II–733. IEEE, 2007. 3
- [49] Marcel Simon, Erik Rodner, and Joachim Denzler. Imagenet pre-trained models with batch normalization. *arXiv preprint arXiv:1612.01452*, 2016. 3
- [50] Karen Simonyan and Andrew Zisserman. Two-stream convolutional networks for action recognition in videos. *Advances in neural information processing systems*, 27, 2014. 7
- [51] Khurram Soomro, Amir Roshan Zamir, and Mubarak Shah. Ucf101: A dataset of 101 human actions classes from videos in the wild. *arXiv preprint arXiv:1212.0402*, 2012. 3, 6, 16

- [52] Swabha Swayamdipta, Roy Schwartz, Nicholas Lourie, Yizhong Wang, Hannaneh Hajishirzi, Noah A Smith, and Yejin Choi. Dataset cartography: Mapping and diagnosing datasets with training dynamics. *arXiv preprint arXiv:2009.10795*, 2020. [6](#)
- [53] Yapeng Tian, Jing Shi, Bochen Li, Zhiyao Duan, and Chenliang Xu. Audio-visual event localization in unconstrained videos. In *Proceedings of the European Conference on Computer Vision (ECCV)*, pages 247–263, 2018. [6](#), [8](#), [14](#), [16](#)
- [54] Grant Van Horn, Rui Qian, Kimberly Wilber, Hartwig Adam, Oisín Mac Aodha, and Serge Belongie. Exploring fine-grained audiovisual categorization with the ssw60 dataset. *arXiv preprint arXiv:2207.10664*, 2022. [2](#), [3](#)
- [55] Limin Wang, Yuanjun Xiong, Zhe Wang, Yu Qiao, Dahua Lin, Xiaoou Tang, and Luc Van Gool. Temporal segment networks: Towards good practices for deep action recognition. In *European conference on computer vision*, pages 20–36. Springer, 2016. [1](#)
- [56] Weiyao Wang, Du Tran, and Matt Feiszli. What makes training multi-modal classification networks hard? In *Proceedings of the IEEE/CVF Conference on Computer Vision and Pattern Recognition*, pages 12695–12705, 2020. [3](#), [7](#), [12](#), [15](#)
- [57] Yake Wei, Di Hu, Yapeng Tian, and Xuelong Li. Learning in audio-visual context: A review, analysis, and new perspective. *arXiv preprint arXiv:2208.09579*, 2022. [1](#)
- [58] Nan Wu, Stanislaw Jastrzebski, Kyunghyun Cho, and Krzysztof J Geras. Characterizing and overcoming the greedy nature of learning in multi-modal deep neural networks. In *International Conference on Machine Learning*, pages 24043–24055. PMLR, 2022. [14](#)
- [59] Jason Yosinski, Jeff Clune, Yoshua Bengio, and Hod Lipson. How transferable are features in deep neural networks? *Advances in neural information processing systems*, 27, 2014. [1](#), [4](#)
- [60] Matthew D Zeiler and Rob Fergus. Visualizing and understanding convolutional networks. In *European conference on computer vision*, pages 818–833. Springer, 2014. [4](#)
- [61] Zhaoyang Zeng, Yongsheng Luo, Zhenhua Liu, Fengyun Rao, Dian Li, Weidong Guo, and Zhen Wen. Tencent-mvse: A large-scale benchmark dataset for multi-modal video similarity evaluation. In *Proceedings of the IEEE/CVF Conference on Computer Vision and Pattern Recognition*, pages 3138–3147, 2022. [2](#)
- [62] Hao Zhang, Feng Li, Shilong Liu, Lei Zhang, Hang Su, Jun Zhu, Lionel M Ni, and Heung-Yeung Shum. Dino: Detr with improved denoising anchor boxes for end-to-end object detection. *arXiv preprint arXiv:2203.03605*, 2022. [1](#), [2](#)
- [63] Yu Zhang, James Qin, Daniel S Park, Wei Han, Chung-Cheng Chiu, Ruoming Pang, Quoc V Le, and Yonghui Wu. Pushing the limits of semi-supervised learning for automatic speech recognition. *arXiv preprint arXiv:2010.10504*, 2020. [1](#), [2](#)
- [64] Hang Zhao, Chuang Gan, Andrew Rouditchenko, Carl Vondrick, Josh McDermott, and Antonio Torralba. The sound of pixels. In *Proceedings of the European conference on computer vision (ECCV)*, pages 570–586, 2018. [6](#)
- [65] Jinxing Zhou, Liang Zheng, Yiran Zhong, Shijie Hao, and Meng Wang. Positive sample propagation along the audio-visual event line. In *Proceedings of the IEEE/CVF Conference on Computer Vision and Pattern Recognition*, pages 8436–8444, 2021. [8](#), [12](#), [14](#)
- [66] Barret Zoph, Golnaz Ghiasi, Tsung-Yi Lin, Yin Cui, Hanxiao Liu, Ekin Dogus Cubuk, and Quoc Le. Rethinking pre-training and self-training. *Advances in neural information processing systems*, 33:3833–3845, 2020. [1](#), [3](#)

A. Analysis of dead channels

A.1. Gradient analysis

Symbol	Meaning
\mathcal{L}	Loss function
M	Mini-batch size
m	Index of the feature map within M mini-batch
$x_{k,m}$	m -th feature map of the k -th channel
$\hat{x}_{k,m}$	m -th normalized feature maps of k -th channel
μ_k, σ_k^2	Mean and variance of the k -th channel
γ_k	Trainable scaling parameter in BN

Table 7. Symbols and their meanings.

During feedback, the gradient back-propagated through Batchnorm [27] layers is

$$\begin{aligned} \frac{\partial \mathcal{L}}{\partial x_{k,m}} &= \frac{\partial \mathcal{L}}{\partial \hat{x}_{k,m}} \cdot \frac{1}{\sqrt{\sigma_k^2}} + \frac{\partial \mathcal{L}}{\partial \sigma_k^2} \cdot \frac{2(x_{k,m} - \mu_k)}{M} \\ &+ \frac{\partial \mathcal{L}}{\partial \mu_k} \cdot \frac{1}{M}, \end{aligned} \quad (5)$$

Every term in the gradient $\frac{\partial \mathcal{L}}{\partial x_{k,m}}$ is multiplied with $\frac{\partial \mathcal{L}}{\partial \hat{x}_{k,m}}$ for

$$\begin{aligned} \frac{\partial \mathcal{L}}{\partial \sigma_k^2} &= \sum_{m=1}^M \frac{\partial \mathcal{L}}{\partial \hat{x}_{k,m}} \cdot (x_{k,m} - \mu_k) \cdot \frac{-1}{2} (\sigma_k^2)^{-\frac{3}{2}}, \\ \frac{\partial \mathcal{L}}{\partial \mu_k} &= \sum_{m=1}^M \frac{\partial \mathcal{L}}{\partial \hat{x}_{k,m}} \cdot \frac{-1}{\sqrt{\sigma_k^2}}. \end{aligned} \quad (6)$$

However, $\frac{\partial \mathcal{L}}{\partial \hat{x}_{k,m}}$ is proportional to γ_k via

$$\frac{\partial \mathcal{L}}{\partial \hat{x}_{k,m}} = \frac{\partial \mathcal{L}}{\partial y_{k,m}} \cdot \gamma_k. \quad (7)$$

As a result, the gradient $\frac{\partial \mathcal{L}}{\partial x_{k,m}}$ is proportional to γ_k , indicating that the abnormal (very small in this) γ_k slows down the back-propagation of gradients. The meanings of the symbols above are in Tab. 7.

A.2. Visualization of dead channels

In this part, we show more examples of the dead channels VGGSound and Imagenet pre-trained Resnet-18 [23] models. We randomly select eight images of different classes from CIFAR-100 and show the corresponding feature maps after the first Conv-BN-ReLU. Considering the layout, the visualization results Fig. 9 and Fig. 10 are in page 17 and 18. All the feature maps produced by the same model always have dead features in the same channels, indicating that these channels are hard to be activated.

B. Training costs of Fusion Tuning

Although our proposed Fusion Tuning strategy divides the original joint training into two stages, it does not double the training costs. We calculate the total FLOPs of joint training and our Fusion Tuning strategy on Kinetics-Sounds, AVE (PSP framework [65]) and UCF-101. As shown in Tab. 8, the total FLOPs of Fusion Tuning strategy are $1.36\times$, $1.56\times$ and $1.40\times$ total FLOPs of joint training on Kinetic-Sounds, AVE and UCF-101 dataset. This is because the fine-tuned uni-modal encoders in stage one could provide effective initialization for the stage two, so that the fusion step would not use as many epoches as the joint learning strategy but bring better performance.

C. Supplementary experiment and analysis

C.1. Effect of ABRi on uni-modal datasets

In this part, we show the performance of the random initialized model, VGGSound pre-trained model and VGGSound pre-trained model with ABRi on Caltech-256 and ESC-50 dataset in Fig. 5. The consistent performance improvement indicates the effectiveness of ABRi on different uni-modal datasets.

We also visualize the filters of the first convolutional layer in VGGSound pre-trained model with and without ABRi after fine-tuning on CIFAR-100. As shown in Fig. 6, many filters in the model without ABRi are still under-optimized after fine-tuning, while most of the filters in the model with ABRi are better updated. This indicates that our ABRi method helps the model to better utilize its capacity.

C.2. Effect of ABRi on ResNet-34

We further apply ABRi on ImageNet and VGGSound pre-trained ResNet-34 [23] models, then evaluate the performance on CIFAR-100 and ESC-50 dataset. The performance improvement shown in Tab. 9 proves that ABRi could be extended to more models other than ResNet-18.

C.3. Effect of Fusion Tuning on uni-modal encoders

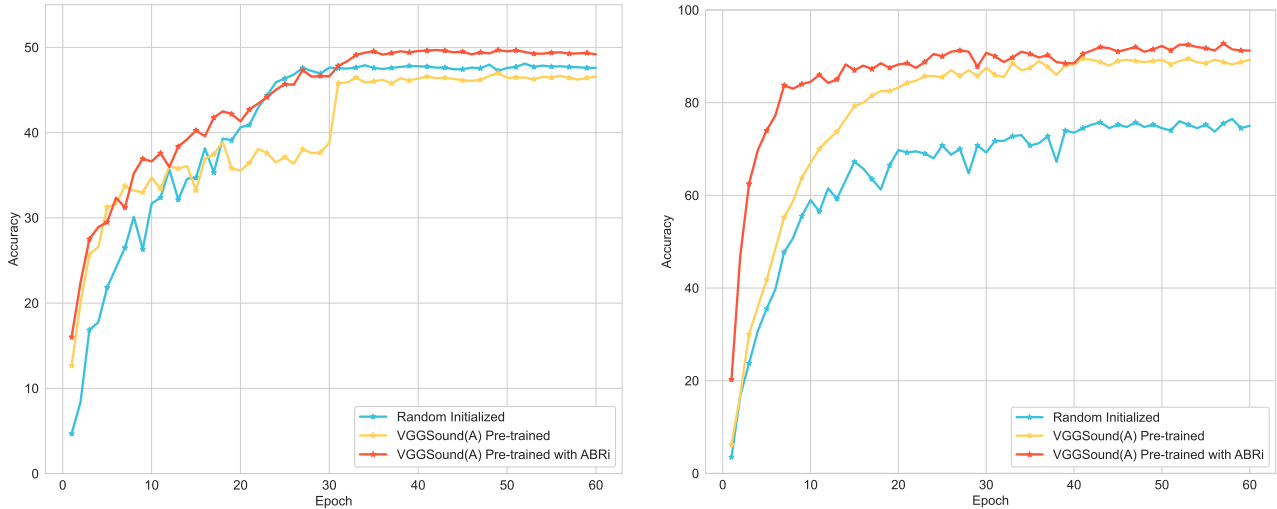
In this part, we show that Fusion Tuning could improve the representation quality of uni-modal encoders and better exploit model knowledge. We compare the accuracy of the multi-modal model and the linear-probing [2] result of the uni-modal in the multi-modal model on joint training and Fusion Tuning. The result shown in Fig. 7 proves the effectiveness of Fusion Tuning.

C.4. More results on VGGSound subset

We compare the Fusion Tuning strategy with the three variants (FusT*, FusT*-lr and FusT-mean) and the two modulation strategies (OGM-GE [43] and Gradient-Blending [56]) on VGGSound subset. The result in Tab. 13 shows superior performance of our sample-wise method.

Dataset	Strategy	FLOPs per epoch	Epochs	Total FLOPs
Kinetic-Sounds	Joint Training	1.02×10^{10}	60	6.15×10^{11}
	Fusion Tuning	Stage 1-Audio: 4.77×10^9	40	8.34×10^{11}
		Stage 1-Visual: 5.48×10^9 Stage 2: 1.02×10^{10}	80 20	
AVE	Joint Training	2.36×10^{10}	50	1.18×10^{12}
	Fusion Tuning	Stage 1-Audio: 5.17×10^9	40	1.84×10^{12}
		Stage 1-Visual: 1.85×10^{10} Stage 2: 2.36×10^{10}	50 30	
UCF-101	Joint Training	1.10×10^{10}	50	5.48×10^{11}
	Fusion Tuning	Stage 1-RGB: 5.48×10^9	20	7.67×10^{11}
		Stage 1-Flow: 5.48×10^9 Stage 2: 1.10×10^{10}	80 20	

Table 8. Comparison of FLOPs on different datasets.



(a) Accuracy of the models on Caltech-256.

(b) Accuracy of the models on ESC-50 fold-5.

Figure 5. **Effect of ABRI on Caltech-256 and ESC-50 dataset.** (a) Performance of random initialized model, VGGSound pre-trained model and VGGSound pre-trained model with ABRI on Caltech-256 testing set. (b) Performance of random initialized model, VGGSound pre-trained model and VGGSound pre-trained model with ABRI on ESC-50 fold-5.

C.5. Integration of the two methods

We make a comparison of applying ABRI for only one encoder or both encoders on AVE and UCF-101 dataset, as shown in Tab. 10 and Tab. 11. The performance on UCF-101 drops when ABRI is applied on both encoders compared with only on optical flow encoder, while the performance on AVE shows an opposite trend. We find that this interesting phenomenon might be associated with the im-

balance of modalities in the dataset, which could be reflected by the uni-modal performance in the first stage to some extent. When applying ImageNet pre-trained model for both modalities, the accuracy of the two modalities in the first stage has a gap on UCF-101 (77.52 for RGB and 66.02 for optical flow). However, this gap is not evident on AVE dataset (59.46 for audio and 58.72 for visual). This indicates that it might be more appropriate to apply ABRI only for the encoder of weaker modality to narrow the im-

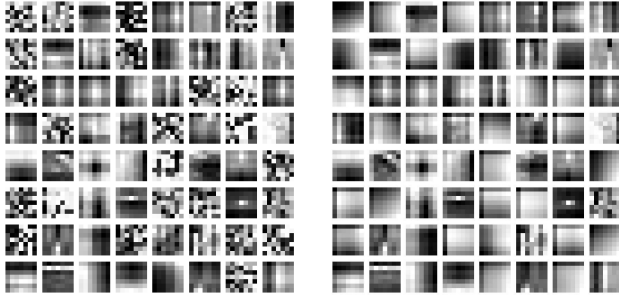


Figure 6. Visualization of the filters in the first convolutional layer of VGGSound pre-trained models with and without ABRi. The models are fine-tuned on CIFAR-100. Left: the model without ABRi. Right: the model with ABRi.

Pre-train	Audio task ESC50	Visual task CIFAR-100
Random	78.55	77.26
ImageNet (V)	89.90	81.67
VGGSound (A)	92.55	75.16
ImageNet (V)†	90.15 (+0.25)	81.89 (+0.22)
VGGSound (A)†	93.80 (+1.25)	77.58 (+2.42)

Table 9. Comparison of performance with and without ABRi on different uni-modal datasets. The backbone is ResNet-34. † indicates ABRi is applied.

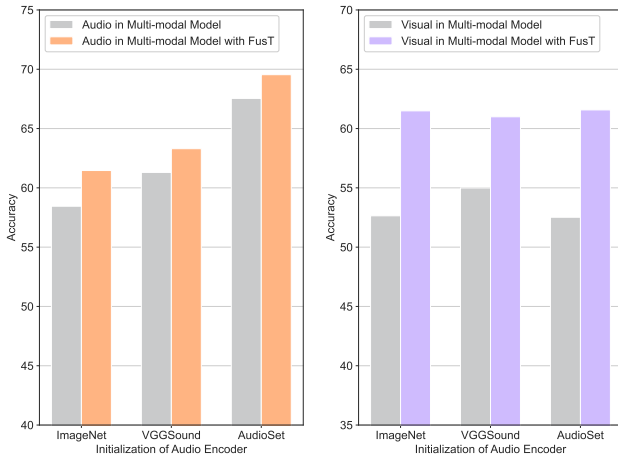


Figure 7. Effect of Fusion Tuning on uni-modal encoders. The experiment is conducted on Kinetics-Sounds dataset. Visual encoders are pre-trained on ImageNet. The accuracy of the uni-modal encoders is obtained through linear-probing.

balance when the gap is evident, while for both encoders when the dataset is more balanced. This strategy is similar to the existing modulation methods which aim to bridge the gap in multi-modal joint training [43, 58].

Framework	Strategy	Pre-train (Audio)	Acc
AGVA [53]	FusT†	VGGSound	71.14
		ImageNet	67.57
	FusT‡	VGGSound	72.64
		ImageNet	68.41
PSP [65]	FusT†	VGGSound	73.43
		ImageNet	69.15
	FusT‡	VGGSound	74.13
		ImageNet	71.89

Table 10. Comparison on AVE dataset with and without Fusion Tuning strategy and ABRi methods in two frameworks. Visual encoders are pre-trained on ImageNet. † indicates that ABRi is applied on visual encoders. ‡ indicates that ABRi is applied on both encoders.

Strategy	Accuracy	mAP
Fusion Tuning†	84.37	89.28
Fusion Tuning‡	83.62	89.00

Table 11. Performance of the model with Fusion Tuning strategy and ABRi on UCF-101. Encoders are pre-trained on ImageNet. † indicates that ABRi is applied on optical flow encoders. ‡ indicates that ABRi is applied on both encoders.

ρ^a	ρ^v	η^a	η^v	t	Accuracy
1.0	0.4	1.0	1.0	0.2	77.59

Table 12. The anchor setting of hyper-parameters of Fusion Tuning.

C.6. Evaluation of hyper-parameter settings

In this part, we test the sensitivity of our Fusion Tuning strategy to different hyper-parameter settings. We choose the setting of the model with ImageNet pre-trained encoders on Kinetics-Sounds dataset shown in Tab. 12 as the anchor. Then, we evaluate the performance of the model when changing one of the hyper-parameters. The results in Fig. 8 indicate that our masking strategy consistently improves the performance under all of these settings. This demonstrates that our Fusion Tuning strategy is not quite sensitive to the hyper-parameter settings.

D. Introduction of datasets

Pre-training datasets. We select three widely used large-scale datasets: ImageNet-1K [12] (visual), VGGSound [8] (audio) and AudioSet [16] (audio) to pre-train our models. Imagenet-1K is an image classification dataset

	Pre-train (Audio)	FusT*	FusT*-lr	FusT-mean	OGM-GE [43]	G-Blending [56]	FusT
Acc	AudioSet	52.66	52.72	52.71	51.28	52.76	52.78
	ImageNet	49.46	49.53	49.31	47.98	49.56	49.62
mAP	AudioSet	55.21	55.42	55.16	54.61	55.25	55.89
	ImageNet	51.13	51.27	51.18	50.42	51.89	52.04

Table 13. Comparison with variants of FusT and two modulation strategies on VGGSound subset. Visual encoders are pre-trained on ImageNet. FusT*, FusT*-lr and FusT-mean are three variants of FusT strategy. * indicates masking strategy is not applied in the second stage.

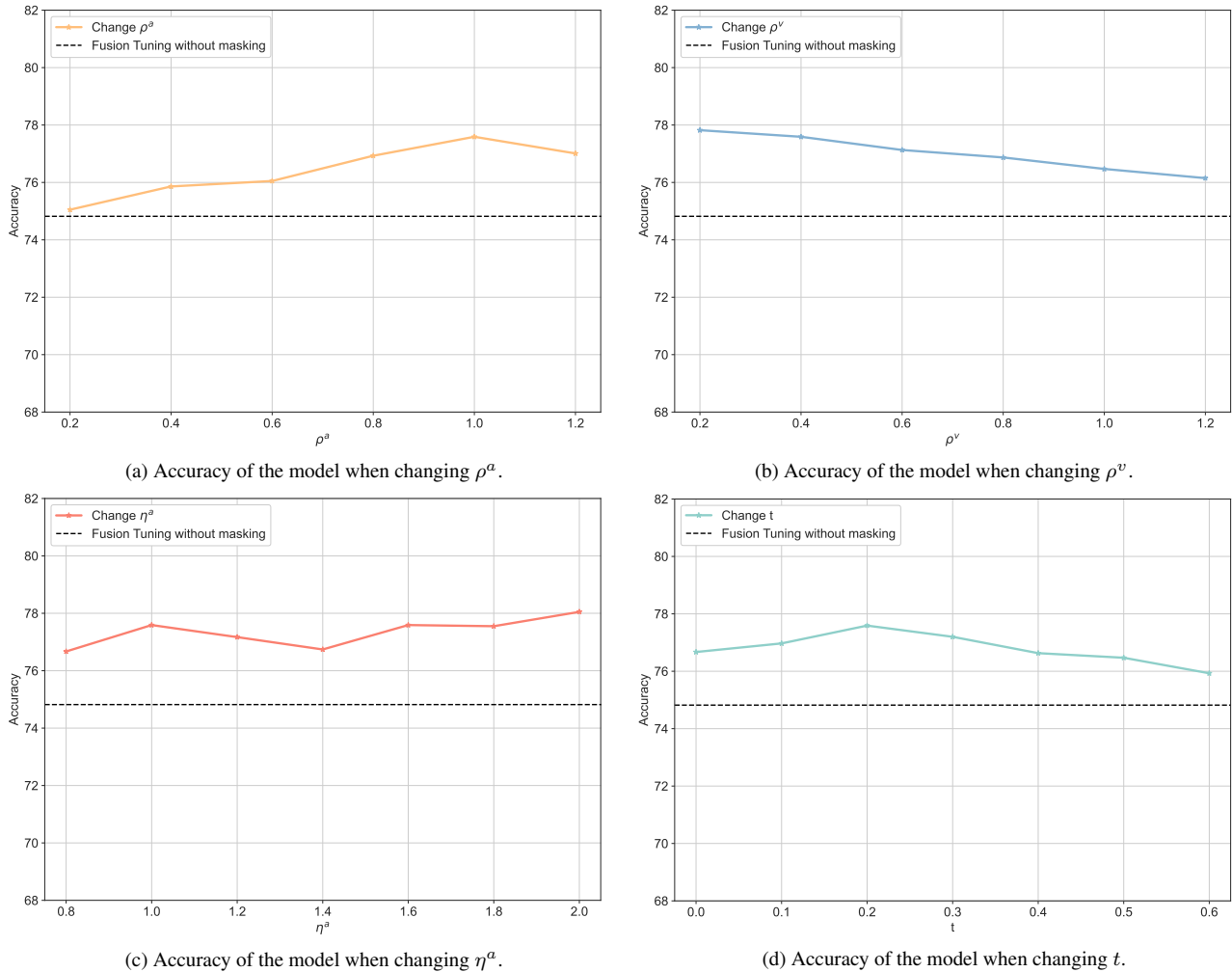


Figure 8. Accuracy of the model with different hyper-parameter settings on Kinetics-Sounds. We evaluate the accuracy when changing ρ^a , ρ^v , η^a and t . One parameter changes while the others remain the anchor value in each experiment. The dashed black line marks the accuracy of Fusion Tuning without masking.

with about 1.28M training images and 50k validation images for 1,000 classes. VGGSound is a video dataset containing 309 classes of audio events in everyday life. We successfully download 91% videos of the full dataset. In our pre-training setting, we extract the audio from 168,618

videos in the training set and 13,954 videos in the testing set. AudioSet is a large-scale video dataset with 602 audio event categories. We use the audio clips of 1,990,695 videos in the training set to pre-train the model and evaluate on 20,285 audio clips in the testing set.

Uni-modal datasets. For audio modality, we use ESC-50 [45] and TUT Acoustic Scenes 2016 [38] datasets. ESC-50 is an audio environment sound classification dataset containing 2,000 audio clips for 50 classes. All the samples are split into five folds and the experiment results are obtained by cross-validation on the five folds. TUT Acoustic Scenes 2016 dataset consists of 6,300 audio clips from 15 acoustic scenes. We train the model on the development set (4,680 samples) and test on the evaluation set (1,620 samples). We also extract the audio modality from Kinetics-Sounds [5] as a uni-modal dataset. For visual modality, CIFAR-100 [33] and Caltech-256 [20] are selected to be the target datasets. CIFAR-100 is a tiny nature image dataset with 100 classes. There is a total of 50,000 images in the training set and 10,000 images in the testing set. Caltech-256 consists of 30,608 images from 256 object categories. The amount of images per category is between 80 and 827.

Multi-modal datasets. For multi-modal tasks, Kinetics-Sounds, AVE [53] and UCF-101 [51] are chosen. Kinetics-Sounds (KS) is a dataset consisting of 31 kinds of human action videos. It contains 15k training samples, 1.9k validation samples and 1.9k testing samples. AVE is an audio-visual event localization dataset with 28 event classes. It contains 4,143 videos of 10 seconds with frame-level annotations. UCF-101 is an action recognition dataset containing 101 categories of action video. It contains RGB and optical flow modality. The total 13,320 videos are divided into a training set with 9,537 samples and a testing set with 3,783 samples. We also randomly select a subset of VG-GSound, where the amount of samples per class is 90,10,30 in the training, validation and testing set.

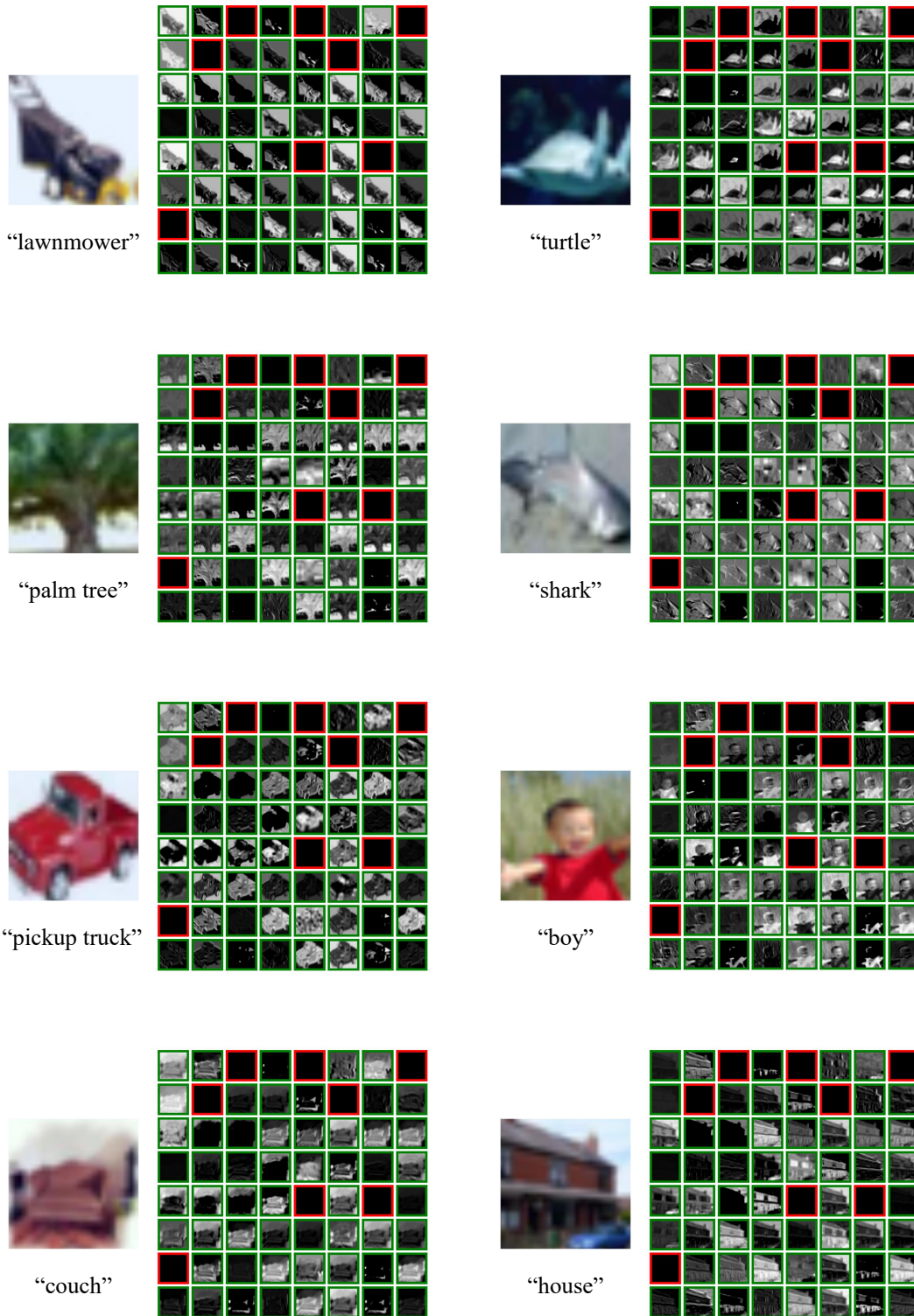


Figure 9. **Visualization of dead channels in ImageNet pre-trained Resnet-18 model.** The input images are randomly selected from CIFAR-100 dataset. For each pair of images, the input is on the left while the feature maps are on the right. The feature maps of the channels marked with red boxes in the figure are dead features and the corresponding Batchnorm parameters are smaller than 2×10^{-5} .

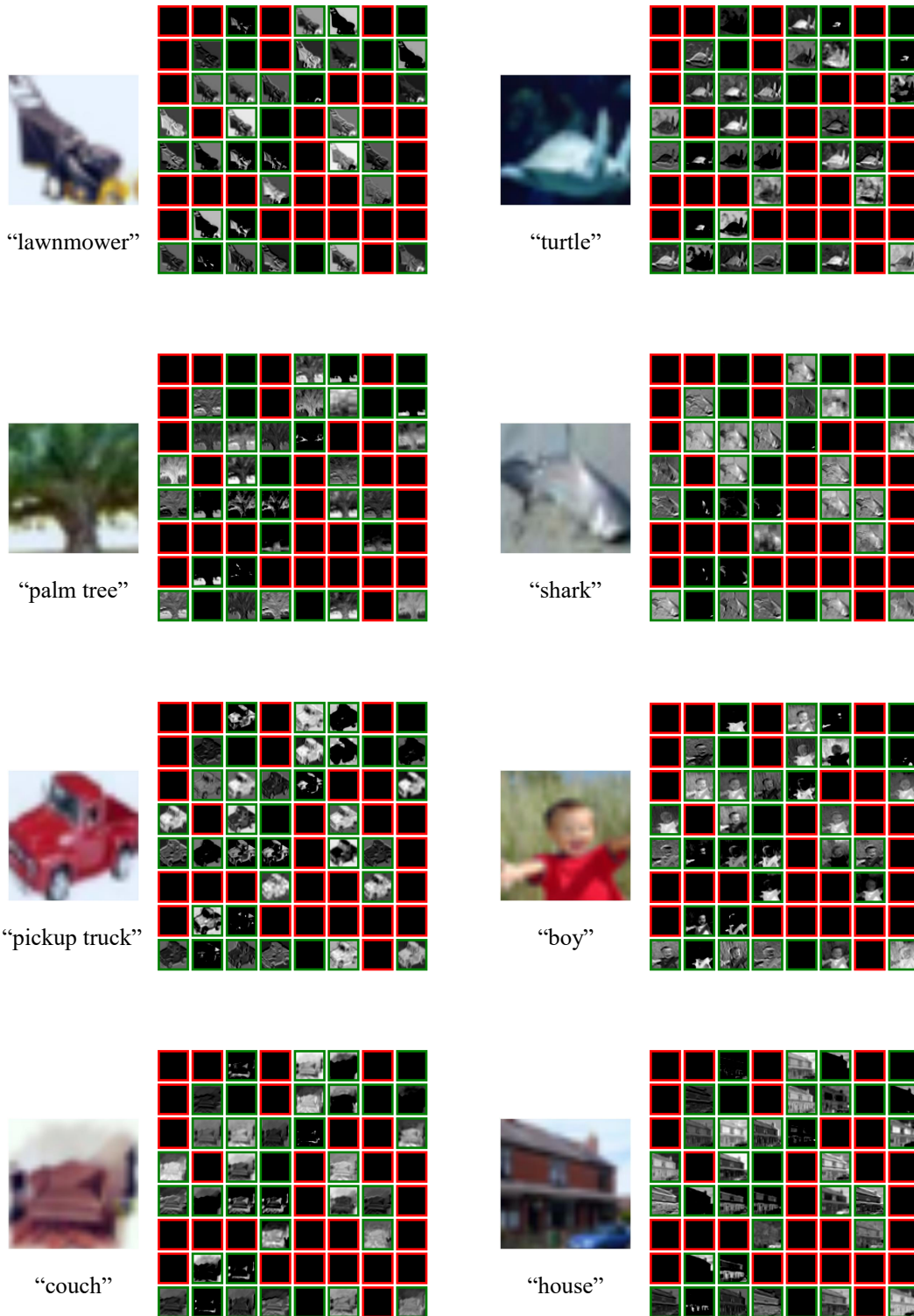


Figure 10. **Visualization of dead channels in VGGSound pre-trained Resnet-18 model.** The input images are randomly selected from CIFAR-100 dataset. For each pair of images, the input is on the left while the feature maps are on the right. The feature maps of the channels marked with red boxes in the figure are dead features and the corresponding Batchnorm parameters are smaller than 2×10^{-5} .